Capacitive Micromachined Ultrasound Transducer (CMUT) for Distance Measurement

***Abstract*— Capacitive Micromachined Ultrasound Transducers (CMUT) have been widely used by the industry owing to its numerous advantages such as easy fabrication process, higher bandwidth, better integration etc. In this project a CMUT cell is designed for distance measurement with frequency in the 100-200 kHz range. The entire design and analysis were performed considering that the CMUT was to be fabricated using PolyMUMPs technology. Various analyses were done using analytical model and FEM model in LTSPICE, MATLAB, and COMSOL that includes- eigenfrequency, frequency response, displacement, collapse voltage, parametric and acoustic analysis. Graphs and results from these simulations showed the CMUT characteristics and confirmed the calculations. Desired result was achieved and compared with the FEM model having minor variation from the analytical model.**

Keywords—CMUT, ultrasound, polyMUMPs, COMSOL, LTSPICE, Micromachine, Circular transducer

I. Introduction

Capacitive Micromachined Ultrasound Transducers or CMUTs is a breakthrough ultrasound technology that has emerged as a viable mechanism for generating stable ultrasound signals. CMUTs are MEMS devices that can generate and receive acoustic signals falling within the ultrasonic range of the spectrum (>20 KHz). They are increasingly being employed in a wide variety of industrial and medical applications such as in microscopy, printer inkjet, portable scanners and many others. In comparison to traditional ultrasound transducers, CMUTs deliver number of advantages such as easier fabrication process for large arrays, large bandwidth and better integration with driver circuitry. They have also recently emerged as a possible substitute to piezoelectric transducers due their advantages mentioned above. The basic structure and typical working modes of a CMUT is shown below [1].

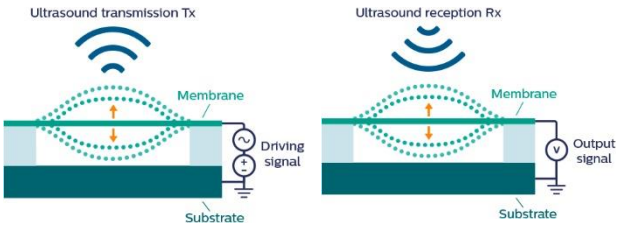


Fig. 1: Basic structure and typical working modes of a CMUT [1].

This project is aimed for the design of a CMUT for range sensor development that would enable the estimation of objects/obstacles close to the sensor using acoustic signals. CMUT cells generally consist of electrodes, diaphragms (membranes), and cavities in a parallel capacitor plate arrangement. When the CMUT is in operation, a DC bias voltage is frequently given to cause the film to sink into the cavity due to the force generated between the parallel plates, increasing the transducer's sensitivity [2]. The AC signal should be superimposed on the applied DC bias voltage when transmitting ultrasound, and the driving frequency of the AC signal then becomes the ultrasound transmission frequency. And on the other hand, the diaphragm is responsible for converting mechanical energy into electrical signals when receiving the ultrasonic signals. For establishing the CMUT based sensor idea, a single element circular CMUT in vacuum can be considered for development and the parameters can be designed as in [3] with a resonance frequency and operational voltage which shall be decided based on commercial standards.

The purpose of this project is to offer an analytic model and electromechanical equivalent circuit for a CMUT, as well as to demonstrate finite element studies of the CMUT cell, including eigenfrequency, frequency response, static, and parametric analysis.

II. Background Study

A. CMUT

Capacitive micromachined ultrasonic transducers (CMUTs), which were first introduced a few decades ago, have proven to be a viable alternative to traditional piezoelectric transducers in terms of sensitivity, transduction efficiency, and bandwidth [4]. A capacitor cell, as shown in Fig. 2 (a), is the basic building block of a CMUT. It consists of a metalized membrane suspended above a heavily doped silicon substrate. As shown in Fig. 2 (b), a single element in the array is made up of many small capacitor cells connected in parallel. Fig. 2 (c) shows a top view of four elements of a 1-D CMUT linear array. A direct current voltage is applied between the metalized membrane and the substrate during CMUT operation. Ultrasound is produced by applying an alternating voltage to the membrane. The capacitance change under constant bias voltage produces a current output when the biased membrane is subjected to ultrasound. The frequency of the incident wave, the bias voltage, and the capacitance of the device all influence the amplitude of this current output [5].

The electrostatic force generated on a capacitor's plates is proportional to the square of the applied voltage, the capacitor's area, and the permittivity of the material between the plates, but inversely proportional to the square of the plate separation:

$$F_{elec} = \frac{\varepsilon_0 S V^2}{2d^2} \qquad (1)$$

where V is the applied bias voltage, S is the area of capacitor plates, ε_0 is the permittivity, and d is the distance between the capacitor plates. Since the electrostatic force is proportional to the square of the bias voltage, linear cMUT operation necessitates the use of both alternating current (AC) and direct current (DC) bias voltages. So, the equation for the electrostatic force will be:

$$F_{elec} = \frac{\varepsilon_0 S}{2d^2}(V_{DC}^2 + 2V_{DC}V_{AC} + V_{AC}^2) \qquad (2)$$

The static force is represented by the first term in parenthesis, the excitation force is proportional to the applied

AC voltage, and the harmonic contribution of the AC voltage is also represented by the last term in parenthesis. The harmonic contribution can be ignored when the DC bias voltage is much higher than the AC excitation voltage [6].

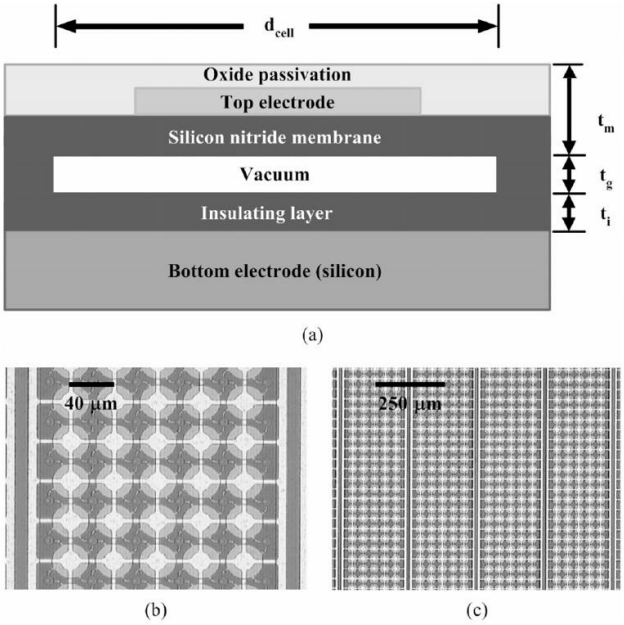


Fig. 2: 1-D CMUT array. (a) Cross section of a CMUT cell. (b) 5-cell wide, 1-D array. (c) A part of four elements of the 1-D CMUT array [5].

B. Comparison: CMUT and PMUT

When the bias voltage is near the device's collapse point, which can range from 30V to 200V depending on the structure, cMUT transducers have a high efficiency [4], [5]. The use of such a high biasing voltage in both the Transmitter (Tx) and Receiver (Rx) modes increases power consumption and necessitates separate high voltage channels in the interface, making cMUTs unsuitable for portable applications. pMUT, on the other hand, does not require a biasing voltage, making it ideal for portable applications. The Piezoelectric Micromachined Ultrasonic Transducer paves the way for ultrasonic diagnosis applications that require low power and voltage [7]. TABLE *1* summarizes the key specifications of cMUT and pMUT devices .

TABLE 1 COMPARISON OF CMUT & PMUT

	CMUT	PMUT
Phenomena	electrostatic transduction	piezoactuation
Excitation voltage	5-30V	2-30V
Bias voltage	30-200	NO BIAS
Typical element size	<100μm x 100μm	>200μm x 200μm
Membrane	Si	Si
Bandwidth	10kHz-10MHz	100kHz-10MHz
Feed thru cap	>200pF	20pF
Receive sensitivity	2mV/kPa	up to 10mV/kPa

High bandwidths and high electromechanical coupling coefficients are two of the most appealing features of the cMUT design for next-generation ultrasonic transducers. Because the spring constant of the two electrode plates can be adjusted using a DC bias, the electromechanical coupling coefficient of cMUT devices can theoretically reach 100%. cMUTs, on the other hand, have some drawbacks in practical applications. For example:

- low ultrasonic intensity due to a limited vacuum gap.
- the requirement of high biasing voltages.
- large power consumption.
- the pull-in effect [8], [9].

pMUTs do not have a vacuum gap between the top and bottom electrodes for vibration, unlike cMUTs. As a result, the membrane's deflection is not limited by the distance between the top and bottom electrodes. Although the pMUT has a number of advantages over cMUTs and piezocomposite transducers, it also has some drawbacks that must be addressed. The coupling coefficient of the pMUT, for example, is quite low. PZT-based piezocomposite ultrasonic transducers and cMUTs have nominal coupling coefficients of 18 percent and 70%, respectively, whereas pMUTs have a coupling coefficient of around 1%–6% [8].

III. ANALYTICAL MODELING OF CMUT

To design the CMUT for this project we have followed the workflow mentioned in the Fig. below.

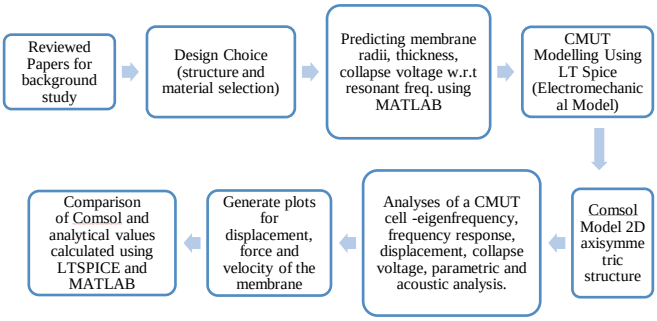


Fig. 3: Workflow for the CMUT designing project

A. Electromechanics Model

Numerous properties of the structure are governed by the CMUT's size parameters. The resonant frequency, the pull-in voltage, and the mechanical impedance are three of the most critical. The first resonance frequency can be estimated by [10]:

$$f_r = \frac{1}{2\pi}\sqrt{\frac{k}{m}} \approx \frac{2t_m}{\pi a^2}\sqrt{\frac{Y_0 + T}{1.8\rho(1-\sigma^2)}} \qquad (3)$$

The pull-in voltage for the structure is approximately given by [11], [12]:

$$V_{col} \approx 0.7\sqrt{\frac{128(Y_0 + T)t_m^3 t_g^3}{27\varepsilon_0(1-\sigma^2)a^4}} \qquad (4)$$

In the above equations, f_r is the resonance frequency, tm is the membrane thickness, tg is the gap between the two conducting surfaces, Y0 is the Young's modulus, T is the intrinsic stress, ρ is the density of the material the conducting surfaces is made of and σ is Poisson's ratio.

The formulas are for structures with a vacuum chamber and no extra insulating layer between the membrane and bottom electrode. Air or other gases within the chamber will give a damping effect on the membrane, and the insulating layer will affect the gap height, and thereby affect both capacitance and gap [13].

The CMUT can be modelled as a capacitor having a capacitance calculated as [11]:

$$C_c \approx 2\pi\varepsilon_0 \int_0^a \frac{r}{t_g - w(r)} dr \qquad (5)$$

In this case w(r) is the deflection of the membrane in a direction perpendicular to the orientation of the membrane, as a function of radial position.

The CMUT turns ratio, or transformer ratio, n, is another important element of a CMUT circuit that gives a measure of its electromechanical conversion between the mechanical and electrical domain [11]:

$$\mathrm{n} = 2\pi\varepsilon_0 \int_0^a \frac{r.dr}{\left(g - x(r)\right)^2} \qquad (6)$$

A dc bias voltage is essential for the correct operation of a CMUT in both the transmission and receiving modes [14]. The deflection of the membrane was computed using the equation:

$$w(r) = \frac{1}{64}\frac{P}{D}(r^2 - a^2)^2 \qquad (7)$$

where P is the pressure on the membrane per area (P= F_e/Area) resulting from the electrical force Fe [13] due to applied bias voltage V and g is the gap between the membrane.

$$F_e = \frac{\varepsilon A V^2}{2g^2} \qquad (8)$$

On the acoustic side, the capacitor with negative capacitance compensates for the spring softening effect caused by electromechanical interaction. The CMUT's complex impedance is represented by the inductor Lm and capacitor Cm on the acoustic side [12].

$$Z_m S = \frac{1}{j\omega C_m} + j\omega L_m \qquad (9)$$

Where Cm = 1/km and Lm = m

$$m = 1.8 t_m \rho \pi a^2 \qquad (10)$$

$$k_m = \frac{16 t_m^3 \pi Y_0}{a^2(1-\sigma^2)} \qquad (11)$$

The acoustical impedance of surrounding medium (air) is modelled as the resistor Ra [12]:

$$Ra = A * v_{sound} * \rho \qquad (12)$$

Where A is the area of membrane, v_{sound} the velocity of sound in air and ρ is the density of the membrane.

B. *Equivalent Circuit Model for CMUT*

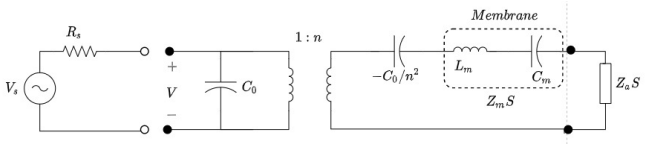


Fig. 4: Equivalent circuit in transmitter mode [12].

It may aid in the calculation of electrical impedance or sensitivity as a function of frequency by capturing small CMUT behaviors in one dimension. Because the CMUT is a reciprocal device, the research is limited to one mode: a small-signal transmitter. The clamp capacitance at bias voltage is represented by model component Co, whereas the spring softening capacitance is represented by model component Cm.

Vs is also a voltage source for input. Mechanical membrane impedance and medium acoustic impedance, respectively, are Zm and Za in the mechanical component. ZaS is modeled as the acoustic impedance of air medium. In the LTSpice simulation it is represented as Ra.

C. *Matlab Calculation & LTSPICE Simulation*

Matlab was used for the prediction of the radius of the membrane, thickness of the membrane, gap of the air medium between the membranes and the range of frequency for the desired resonant frequency. Graphs were plotted for finding the values. Further explanation is given in the Matlab Calculations result section.

The CMUT was originally modeled as a lumped electro-mechanical model with a spring, mass, and parallel plate capacitor. As illustrated in Fig. 5, this resulted in an equivalent circuit for a two-port network with an electrical domain at one port and an acoustic mechanical domain at the other. Mason's electrical equivalent circuit model for an electroacoustic transducer was used to analyze the CMUT transducer [15].

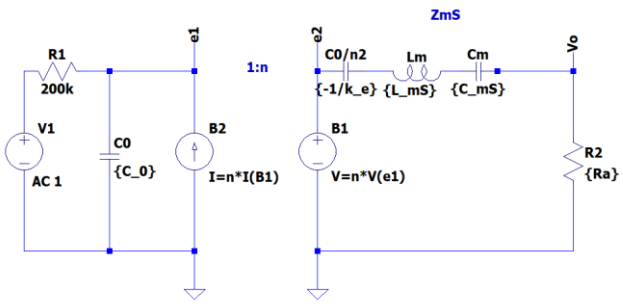


Fig. 5: Schematic of lumped circuit model of CMUT

The parameters used for the LTSPICE model have been tabulated in TABLE 2.

TABLE 2 PARAMETERS USED IN LTSPICE MODEL

Parameter	Value
Turns ratio, n	1.8673e-05
Capacitance, Co	6.8399e-13 F

Capacitance, Cm	3.2527e-04 F
Inductance, Lm	3.0857e-09 H
Membrane stiffness, Km	3.0743e+03
Acoustic impedance, Ra	1.61e-6 Ω
Softening constant, Ke	509.7469
Young's modulus for the membrane, Yo	169e9 N/m2
Poisson's ratio for the Membrane, σ	0.22
Sound speed in the air	330 m/s
DC Bias voltage for frequency response, Vdc	100 V
Air permittivity, ε_0	8.85418782e-12
Membrane density	2320 g/cm3

IV. MATERIALS AND MODEL SELECTION

A. Material

The polyMUMPs procedure lays the groundwork for designing a polyMUMPs structure. A set of design process rules is a crucial aspect of the setup. These guidelines apply to the materials that should be used in the fabrication process, as well as the varied layer thicknesses that can be used. Polysilicon, silicon oxide, silicon nitride, and metal are among the materials used in the polyMUMPs process. These materials are used for a variety of purposes during the procedure. Underneath the first polysilicon layer, nitride is employed as an insulating layer [16]. After that, the structure can be built up of multiple layers of silicon oxide and polysilicon, with silicon oxide serving as a sacrificial layer as shown in Fig. 2.

For this analysis, typical values [16] for length of the membrane and thickness of different part were implemented at the beginning which were modified later on based on the formulated calculation and LTSpice equivalent circuit modelling which are being illustrated in TABLE 3.

TABLE 3 IMPLEMENTED PARAMETERS FOR CMUT

Parameter	**Values (µm)**
Membrane thickness, tm	3
Gap Thickness, go	3.5
Bottom polysilicon thickness	3
Radius of the membrane, a	286
Insulator thickness	2.5

The model is designed on the insulating layer base and silicon substrate with the help of COMSOL. Firstly, the radius of the membrane was finalized. For this analysis, the goal was to obtain 100-200 KHz eigenfrequency with an acceptable pull in voltage. Different study and simulation were carried out on the designed typical model [16] from which it was found that the eigenfrequency is inversely proportional to the radius of the membrane. Therefore, after thorough analysis and consideration the radius of the membrane was chosen to be 280 µm. Later on, different parameters were set using LT-Spice equivalent modelling from which the values tabulated in TABLE 2 were estimated. It was evident that the thickness of the membrane affects the model as the radius of the membrane increases and as a result the eigenfrequency increases along with the membrane thickness. The thickness shown above were estimated in order to obtain the desired range of eigenfrequency. As for the gap thickness, during the value estimation phase in MATLAB modelling we obtained Fig. 7 and Fig. 8 which illustrates the relation between eigenfrequency, membrane thickness and pull in or collapse voltage with different radius and gap thickness modelling. The radius of the membrane is related to the collapse voltage and increasing the radius eventually decreases the voltage value and in order to overcome the situation the gap thickness plays a good role. For this model specifically, it was determined that the thickness of gap must be more than 3 µm to keep the spring constant, K valid with respect to the radius of 286 µm. Otherwise, the system collapses much earlier than expected.

B. COMSOL Model

The proposed structure for the CMUT was built in COMSOL Multiphysics in 2D axisymmetric as shown in Fig. 6.

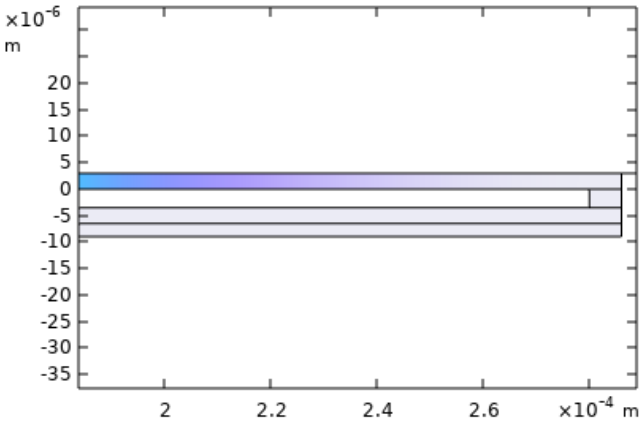


Fig. 6: Proposed CMUT model structured in COMSOL

The 2D structure CMUT was 2D axisymmetric to make it a circular shaped CMUT. In this model, the topmost layer is the polysilicon membrane. After that there is air in the white-colored region along with silicon oxide pillars in the corner. This is the only deforming region of the structure, and this also connects the membrane to the rest of the structure while also insulating it from the lower conducting substance. Then comes the second polysilicon layer which is used as conductors along with the top membrane. At last, the bottom layer of the structure is silicon nitride which works as an insulator. The structure is subject to several constraints. The membrane has free constraints, while the bottom and right boundaries have fixed constraints. Both the nitride and oxide were set to charge conservation, solid type, while the air was tuned to charge conservation, nonsolid type, when it came to electrostatics. The charge on all exterior borders was set to zero. For frequency experiments, the membrane and the bottom polysilicon were made to be terminals, with harmonic perturbation on the bottom one.

Several measurements were made for this model. The displacement was computed using a stationary model at a bias voltage of around 80% of the expected collapse voltage of 126V. Other investigations were conducted to determine the

structure's eigenfrequency, both with and without bias. A parametric sweep from 0 to bias voltage was used in the bias research. A study was also conducted in order to determine the pull-in voltage. The maximum voltage was varied until an error appeared in this study's auxiliary sweep over many voltages. Finally, a frequency response analysis was conducted, with graphs depicting the displacement, force, and velocity of the membrane at various frequencies included in the results.

V. Results & Anaysis

A. *Matlab Calculations & Graphs*

The papers that we have gone through for the applications of CMUT were mostly for medical and fluid applications. In this regard, the frequency was in the megahertz range. Also, the radius, thickness of membrane and gap between the membranes were important aspects to consider for our desired application of the distance measurement in the kilohertz range. To predict the radius of the membrane with varying thickness and also to calculate the collapse voltage we have done analysis in MATLAB. Initially, we planned to use resonant frequency range of 100-200 kHz. Electromechanics Model section explained the set of equations used for the calculation of the values.

In Fig. 7 it can be seen that, the length of radius is inversely proportional to the frequency. As can be seen from the graph, for 150kHz resonant frequency the radius of membrane is approximately 286µm for membrane thickness of 3µm and air gap of 3.5µm. From these values of the graphs, we selected 286µm radius value, membrane thickness of 3µm and air gap of 3.5µm for our FEM analysis in COMSOL.

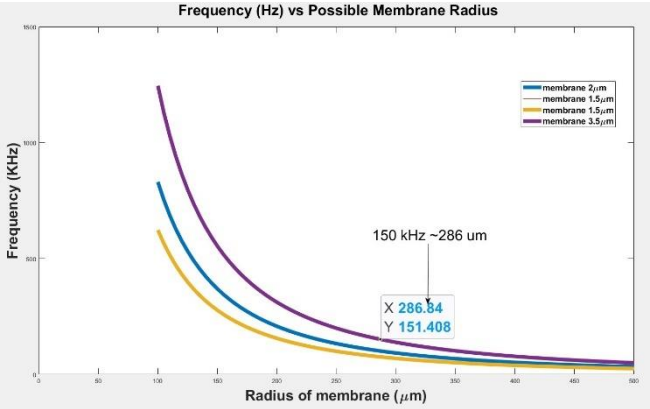


Fig. 7: Graph for resonant frequency vs membrane radius for predicting the range

The collapse voltage in Fig. 8 was also calculated using MATLAB and was found to be around 126 V. From the graph it can be seen that the collapse voltage increases with the thickness of the membrane and also with the increase of the frequency.

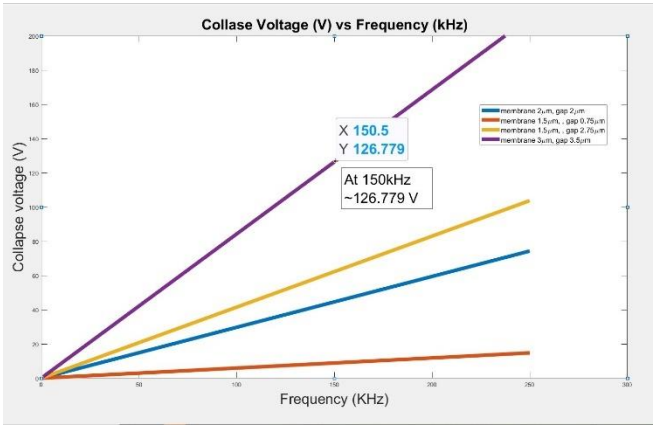


Fig. 8: Graph for collapse voltage vs resonant frequency

B. *LTSPICE & COMSOL Analysis*

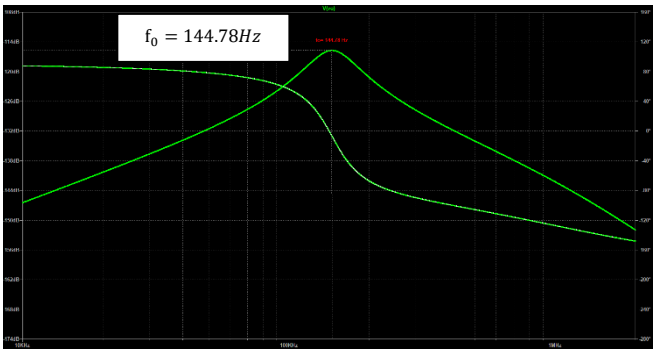


Fig. 9: Resonance frequency generated by LTSPICE

The small signal AC behavior of the CMUT cell around a dc voltage of 100 V and ac voltage of 0 dBm was obtained through LTSpice AC analysis as shown in Fig. 9. The resonant frequency peak was observed at 144.78 kHz i.e ~145kHz. From the COMSOL analysis the first natural resonant frequency is found to be 150.079 kHz which is being illustrated in the point graph Fig. 12.

The COMSOL tool generates various graphs from the structure, with some graphs being almost identical for several experiments. As a result, the plots shown here are the graphs made, as well as one of each of the plots created many times.

TABLE 4 RESULTS FROM LTSPICE & COMSOL

Parameter	COMSOL Value	Calculated/ LTSPICE Value
Collapse Voltage	~114V	~126V
Bias voltage, Vdc	-	100V
Unbiased Eigenfrequency, fo	150.08kHz	145.10kHz
Displacement from center	4.5nm	-

The CMUT cell, is simulated inside a sealed cavity without the bias voltage. Fig. 10 shows that for the chosen structure the deflection is 4.5nm for circular membrane at approximate Eigen frequency of 150 KHz. Even if the membrane was not biased, the difference in pressure between the ambient and the pressure inside the sealed cavity would cause the membrane and top electrode to deflect [17].

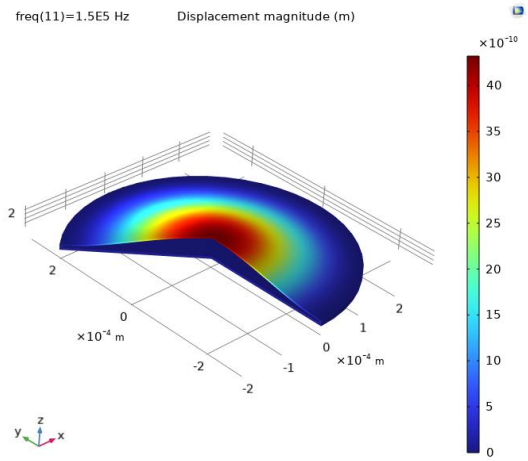


Fig. 10: First natural frequency generated by COMSOL for displacement magnitude

Fig. 11 represents the displacement of the transducer membrane which acts like a cantilever fixed at the silicon oxide pillar contact point and free to move at the other. The minimum displacement at the point of contact to oxide pillar and maximum displacement at membrane center (at axis of symmetry) is plotted.

In Fig. 12 it shows the maximum displacement of the membrane with respect to the frequency. The peak of the frequency is at ~150kHz similar to the other eigenfrequencies.

A parametric sweep of bias voltage was also performed as shown in Fig. 13 and the study gave non-converging values beyond 114V which was estimated as the pull-in or collapse voltage of the system. It depicts the displacement of an illustrative membrane caused by the introduction of DC or bias voltage. While the displacement varies depending on the properties of the materials and their geometries, it can be shown that as the voltage is increased, the membrane displaces in a non-linear manner for fixed materials and geometries corresponding to the proposed model of this research.

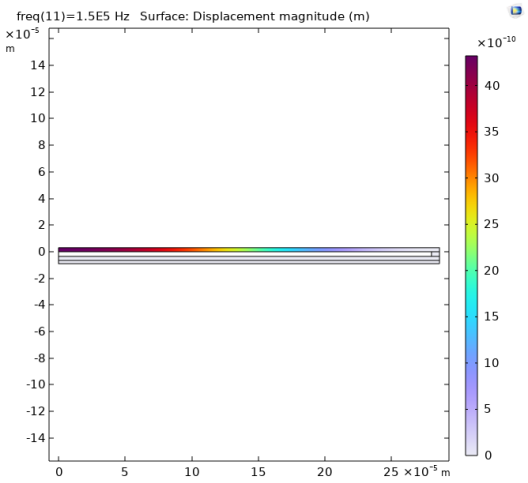


Fig. 11: Surface displacement plot from COMSOL simulation

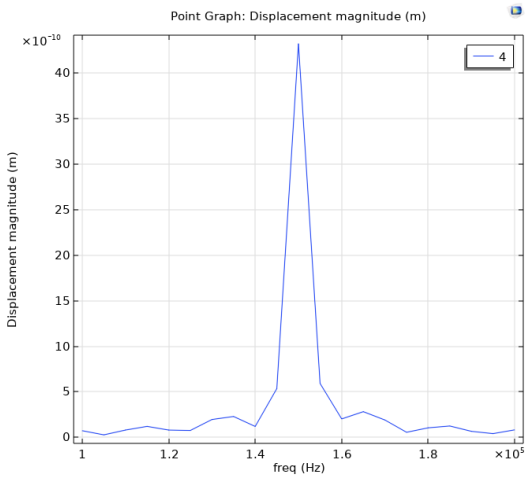


Fig. 12: Graph for max displacement vs frequency

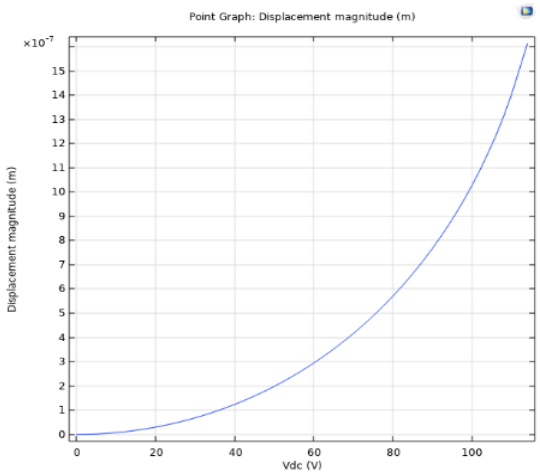


Fig. 13: Plate displacement with respect to bias voltage

When the computed numbers are compared to the values from the models, it is clear that there is a disparity. These are most likely the result of simplifications made when formulae for computations were derived from reference articles. The COMSOL program solves the equations using the FEM model by dividing the structure and doing the computations on each component, effects that are neglected in the one-piece model used to derive the equations are taken into consideration. This will be discussed in further depth further down. The equation for the membrane's resonant frequency has boundary condition that the membrane being fixed at its edge. While this is also true in the COMSOL model, the membrane is resting on the oxide in a manner. As a consequence, the boundary may be seen as somewhat different than when generating the resonant frequency model, resulting in the tiny variation in resonant frequency.

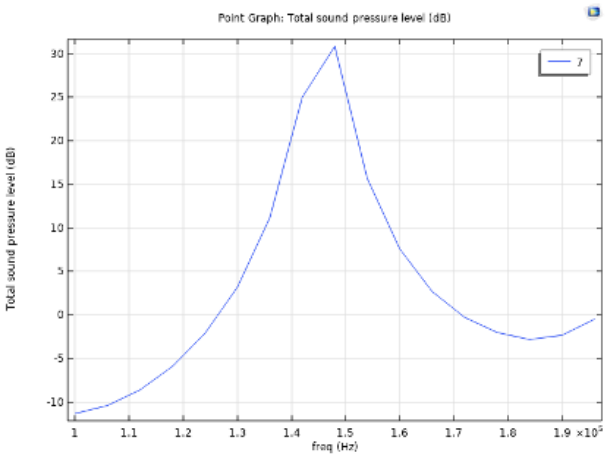
Another factor that simplifies the calculation of the resonant frequency is the fact that the electrical force is constant throughout the whole membrane. The effect is purely indirect, since the force is eliminated when determining the spring constant and mass expressions. However, the simplification altered the formula for the beam's bending, which in turn altered the mass and spring constant expressions. Another factor that may have

significantly altered these two values, and therefore the resonant frequency, is the elimination of the latter terms from the impedance equation. Due to the fact that the initial terms have the most impact, the last terms from the equation are omitted. However, overall, this may result in a slight variation in the predicted and simulated resonance frequency.

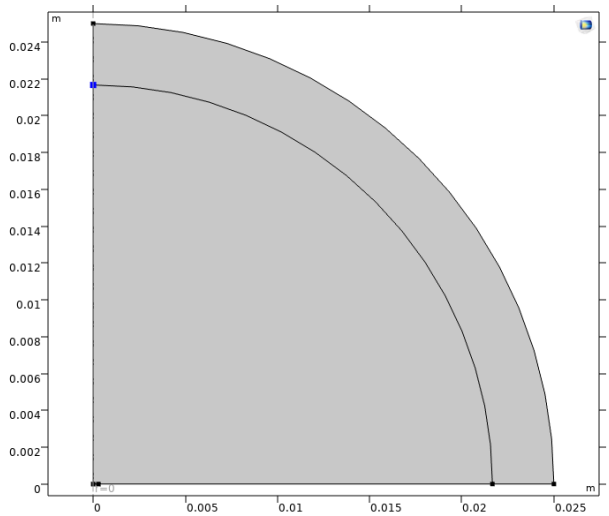
Additionally, the simulated pull-in voltage is different from the calculated value. Though this might be due to programmatic issues, since this was experienced, it is more than likely due to the simplifications used to derive the equation from the reference papers. The resonant frequency was used to demonstrate some of these simplifications. Moreover, the pull-in voltage calculation includes a correction factor that adjusts for beam bending. This is merely a rough estimate, and some mistake is likely as a result. Also, the calculations to determine the pull-in voltage are based on static study, but the spring constant utilized in the formula is based on dynamic analysis, which might account for part of the error.

C. CMUT Acoustic Characterization

The Capacitive MUT construction process involves a vast number of phases with varying structural constraints and materials. Both these properties influence the qualities of the transducer that is produced. As a result, the CMUTs acoustic properties must be identified. The acoustic study of the CMUT was performed in COMSOL using the frequency domain pressure acoustic physics. Since axial symmetry was used for modelling the CMUT, the surrounding medium selected to be of circular geometry was modelled around the transducer using air as the material. The speed of sound in air used for the study was 330m/s, a perfectly matched layer was created at the boundary of the medium and far-field integral approximation was mapped for exterior field calculation. A perfectly matched layer (PML) is a region (also known as a sponge layer) which is applied to an acoustic model to simulate an infinite, unrestricted, non-reflecting domain, generally used to truncate the computational regions. Analogous to nonreflecting border constraints, this layer creates a perfectly absorbing domain. Not only can the PML function with plane waves, but it also works with other sorts of waves. It is also effective at very oblique incidence angles. In the frequency domain, the PML applies a complex-valued coordinate transformation to the chosen domain, effectively rendering it absorbent at a constant wave impedance and removing reflections at the boundary. In the time domain, the inverse Laplace transformed equations are solved for in the PML [18], [19].



a)

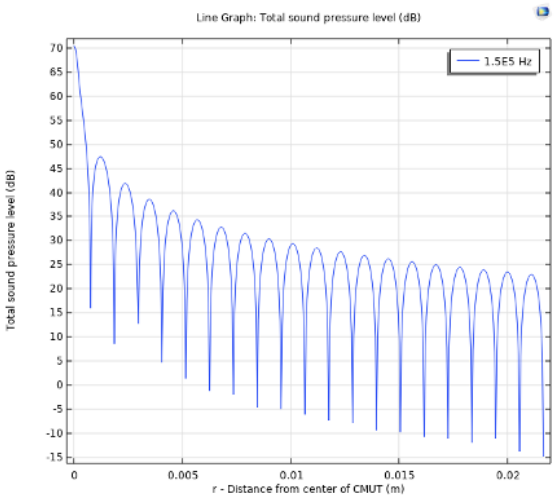


b)

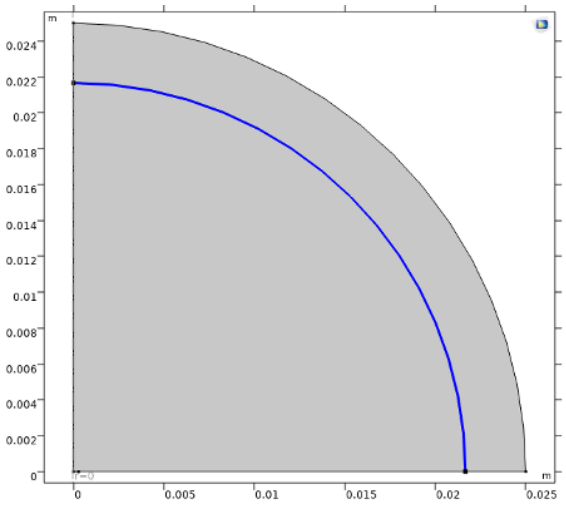
Fig. 14: a) Change in sound intensity of CMUT with frequency sweep and b) its corresponding measurement location

Primarily two important analyses were conducted for acoustic characterization. The first study was to plot the variation in sound intensity with respect to the frequency sweep of the transducer membrane at a fixed bias voltage of 100V. This bias voltage for study was chosen to be around 80% of the analytically calculated collapse or pull-in voltage of the device, which was previously shown to be 126V [20]. Quality factor of 200 was used for the study and isotropic loss factor damping was applied equivalent to 1 over Q factor. As displayed by the graph the total sound pressure depicted in dB of the transducer measured at the edge of the air to PML boundary increased with rising frequency and peaked at the resonance frequency. This indicates that the model output is consistent with the requirement and maximum ultrasound output would be at its eigen frequency. The second study was to plot the variation in sound intensity with respect to the variation in distance from the transducer. The output of this study showed peak intensity very close to the transducer (about 0 arc-length) and diminishing intensity away from the center, rendering the results true to expected behavior as discussed previously about the attenuation of sound amplitude in air. Actual attenuation is dependent on several factors such as the ambient temperature, humidity and so on. Hence the analysis here is not exhaustive nor is it indented towards a detailed study of sensor output attenuation. The

modelled acoustic pressure in the medium at resonance frequency is also shown in 2D and 3D plots. The pressure variations across the medium towards the PML are visible in different color contrasts.

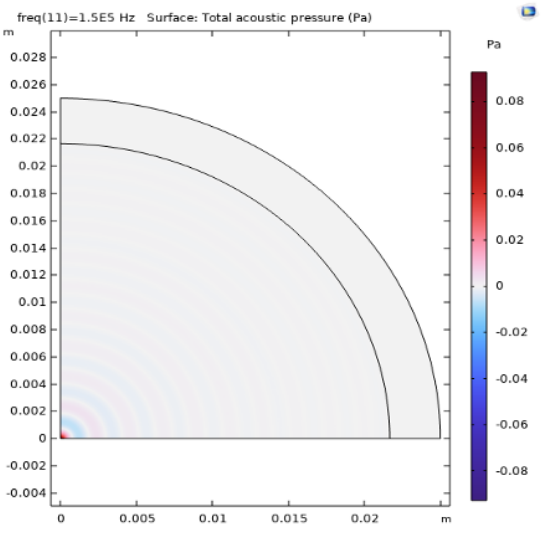


a)

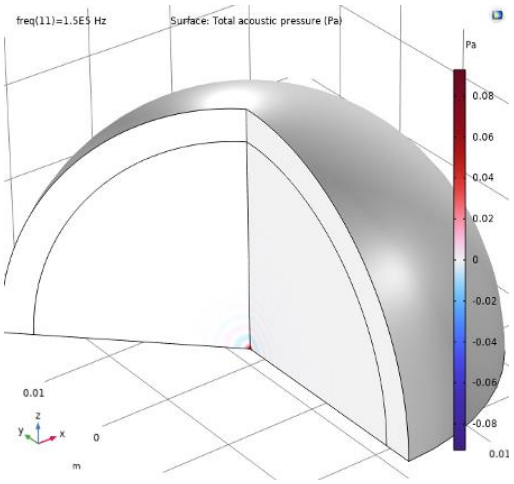


b)

Fig. 15: a) Change in sound intensity of CMUT with distance from center and b) its corresponding measurement location



16 a)



16 b)

Fig. 16: Acoustic pressure variation across the medium at resonance frequency in a) 2D and b) 3D

VI. Conclusion & Perspective

The CMUT has design manufactured using the POLYMUMPs standard method, with a top membrane constructed of polysilicon. Following analysis of several geometrical parameters in terms of membrane thickness, gap thickness, and membrane radius our model is implemented in COMSOL and LTSPICE using $t_m = 3.\mu m, g_0 = 3.5\mu m \; and \; a = 286\mu m$ to create a 150kHz natural frequency. Furthermore, a small-signal equivalent circuit can approximate the device's frequency response and interaction with electronics, providing findings within 4% of the FEM analysis (with 150.08 and 145.10 kHz, respectively). For the analysis of collapse voltage, we obtained V_{pi} at 114V with FEM analysis and 126V with the analytical method that has a 9.5% difference.

Numerous variables affect the resonance frequency and collapse voltage of CMUT. Several key factors from the simulation may be taken into account in order to optimize the device's performance.

- For smaller softening constant (κ_e) and larger membrane stiffness (k_m), the obtained resonance frequency (f_0) is higher.
- Collapse voltage is proportional to the membrane stiffness, i.e is with thicker membrane the collapse voltage increases.
- Acoustic medium properties such as temperature, relative humidity, ambient pressure, and damping factors may be better matched to application.

Additionally, it is evident from the findings that the analytical model with correction numbers (Eq. 4), which are computed with the capacitor's circular form in mind, may give an accurate forecast for the collapse voltage and displacement.

To summarize, small-signal equivalent circuit or spring-mass system provide a correct approximation of the resonance frequency and collapse voltage to predict the CMUT's behavior. If the shape function, operating modes, or complex radiation impedance are incorporated, the lumped model's

accuracy may be increased. Meanwhile, for multi-physics systems like CMUT, FEM modeling is a perfect option. When compared to the analytical technique, its simulation delivers a more reliable and thorough result.

ACKNOWLEDGMENT

The authors would like to thank Associate Professor Hamed Salmani at the Department of Microsystems, USN for his guidance and supervision of the project.

REFERENCES

[1] "Capacitive micromachined ultrasonic transducers | Philips Engineering Solutions." https://www.engineeringsolutions.philips.com/looking-expertise/mems-micro-devices/mems-micro-devices-applications/capacitive-micromachined-ultrasonic-transducers-cmut (accessed May 01, 2022).

[2] B. G. Jeong, D. K. Kim, S. W. Hong, S. W. Chung, and H. J. Shin, "Performance and reliability of new CMUT design with improved efficiency," *Sensors Actuators A Phys.*, vol. 199, pp. 325–333, Sep. 2013, doi: 10.1016/J.SNA.2013.06.001.

[3] H. Köymen *et al.*, "An improved lumped element nonlinear circuit model for a circular CMUT cell," *IEEE Trans. Ultrason. Ferroelectr. Freq. Control*, vol. 59, no. 8, pp. 1791–1799, 2012, doi: 10.1109/TUFFC.2012.2383.

[4] A. S. Ergun, ; Goksen, G. Yaralioglu, and B. T. Khuri-Yakub, "Capacitive Micromachined Ultrasonic Transducers: Theory and Technology", doi: 10.1061/ASCE0893-1321200316:276.

[5] Ö. Oralkan *et al.*, "Capacitive micromachined ultrasonic transducers: Next-generation arrays for acoustic imaging?," *IEEE Trans. Ultrason. Ferroelectr. Freq. Control*, vol. 49, no. 11, pp. 1596–1610, Nov. 2002, doi: 10.1109/TUFFC.2002.1049742.

[6] M. S. Salim, M. F. Abd Malek, R. B. W. Heng, K. M. Juni, and N. Sabri, "Capacitive Micromachined Ultrasonic Transducers: Technology and Application," *J. Med. Ultrasound*, vol. 20, no. 1, pp. 8–31, Mar. 2012, doi: 10.1016/J.JMU.2012.02.001.

[7] J. Tillak and J. Yoo, "A 23μW digitally controlled pMUT interface circuit for Doppler ultrasound Imaging," *Proc. - IEEE Int. Symp. Circuits Syst.*, vol. 2015-July, pp. 1618–1621, Jul. 2015, doi: 10.1109/ISCAS.2015.7168959.

[8] J. Jung, W. Lee, W. Kang, E. Shin, J. Ryu, and H. Choi, "Review of piezoelectric micromachined ultrasonic transducers and their applications," *J. Micromechanics Microengineering*, vol. 27, no. 11, p. 113001, Sep. 2017, doi: 10.1088/1361-6439/AA851B.

[9] J. H. Lee, I. J. Cho, K. Ko, E. S. Yoon, H. H. Park, and T. S. Kim, "Flexible piezoelectric micromachined ultrasonic transducer (pMUT) for application in brain stimulation," *Microsyst. Technol.*, vol. 23, no. 7, pp. 2321–2328, Jul. 2017, doi: 10.1007/S00542-016-2912-5/FIGURES/9.

[10] L. Liang, Y. Li, and P. Zhang, "Modelling and analysis of bandwidth on CMUTs for medical imaging," *IOP Conf. Ser. Mater. Sci. Eng.*, vol. 768, no. 5, Mar. 2020, doi: 10.1088/1757-899X/768/5/052102.

[11] S. Olcum, M. N. Senlik, and A. Atalar, "Optimization of the Gain-Bandwidth Product of Capacitive Micromachined Ultrasonic Transducers," *IEEE Trans. Ultrason. Ferroelectr. Freq. Control*, vol. 52, no. 12, pp. 2211–2219, 2005, doi: 10.1109/TUFFC.2005.1563264.

[12] M. R. Sarder, "(3) (PDF) Design and Modelling of a Single Element CMUT Using POLYMUMPs Process," 2020. https://www.researchgate.net/publication/351075648_Design_and_Modelling_of_a_Single_Element_CMUT_Using_POLYMUMPs_Process (accessed May 03, 2022).

[13] S. D. Senturia, "Microsystem design," p. 689, 2001.

[14] J. D. Fraser, Fraser, and J. Douglas, "Capacitive micromachined ultrasonic transducers," *ASAJ*, vol. 113, no. 3, pp. 1194–1194, 2003, doi: 10.1121/1.1566314.

[15] W. P. Mason, *Electromechanical Transducers and Wave Filters. Second Edition: Mason, Warren P.: 9780442051648: Amazon.com: Books*. 1948. Accessed: May 04, 2022. [Online]. Available: https://www.amazon.com/Electromechanical-Transducers-Wave-Filters-Second/dp/0442051646

[16] A. Cowen, B. Hardy, R. Mahadevan, and S. Wilcenski, "PolyMUMPs Design Handbook a MUMPs® process," 1992.

[17] W. Zhang, H. Zhang, F. Du, J. Shi, S. Jin, and Z. Zeng, "Pull-In Analysis of the Flat Circular CMUT Cell Featuring Sealed Cavity," *Math. Probl. Eng.*, vol. 2015, 2015, doi: 10.1155/2015/150279.

[18] C. Ge and E. Cretu, "Design and fabrication of SU-8 CMUT arrays through grayscale lithography," *Sensors Actuators A Phys.*, vol. 280, pp. 368–375, Sep. 2018, doi: 10.1016/J.SNA.2018.08.006.

[19] "Choosing an Ultrasonic Sensor for Proximity or Distance Measurement -- Part 1: Acoustic Considerations | Fierce Electronics." https://www.fierceelectronics.com/components/choosing-ultrasonic-sensor-for-proximity-or-distance-measurement-part-1-acoustic-0 (accessed May 04, 2022).

[20] R. Boubenia, P. Le Moal, G. Bourbon, E. Ramasso, and E. Joseph, "CMUT-Based Sensor for Acoustic Emission Application: Experimental and Theoretical Contributions to Sensitivity Optimization," *Sensors 2021, Vol. 21, Page 2042*, vol. 21, no. 6, p. 2042, Mar. 2021, doi: 10.3390/S21062042.